

# Mechanisms of magnetoelectricity in manganese doped incipient ferroelectrics

R.O. KUZIAN<sup>1</sup>, V.V. LAGUTA<sup>1,2</sup>, A.-M. DARÉ<sup>3</sup>, I.V. KONDAKOVA<sup>1</sup>, M. MARYSKO<sup>2</sup>, L. RAYMOND<sup>3</sup>, E.P. GARMASH<sup>1</sup>, V.N. PAVLIKOV<sup>1</sup>, A. TKACH<sup>4</sup>, P. M. VILARINHO<sup>4</sup> and R. HAYN<sup>3</sup>

<sup>1</sup> *Institute for Problems of Materials Science NASU - Krzhizhanovskogo 3, 03180 Kiev, Ukraine*

<sup>2</sup> *Institute of Physics, AS CR - Cukrovarnicka 10, 16253 Prague, Czech Republic*

<sup>3</sup> *Aix-Marseille Université, IM2NP CNRS - FST St-Jérôme, Avenue Escadrille Normandie Niemen, F-13397, Marseille Cedex, France*

<sup>4</sup> *Department of Ceramics and Glass Engineering, CICECO, University of Aveiro - 3810-193 Aveiro, Portugal*

PACS 75.85.+t – Magnetoelectric effects, multiferroics

PACS 75.30.Hx – Magnetic impurity interactions

PACS 76. – Magnetic resonance

**Abstract.** - We report magnetization measurements and magnetic resonance data for SrTiO<sub>3</sub> doped by manganese. We show that the recently reported coexistent spin and dipole glass (multiglass) behaviours are strongly affected by the distribution of Mn ions between the Sr and Ti sites. Motivated by this finding we calculate the magnetic interactions between Mn impurities of different kinds. Both LSDA+*U* and many-body perturbation theory evidence that magnetic and magnetoelectric interactions are mediated by Mn<sub>B</sub><sup>4+</sup> ions substituting for Ti. We propose two microscopic magnetoelectric coupling mechanisms, which can be involved in all magnetoelectric systems based on incipient ferroelectrics. In the first one, the electric field modifies the spin susceptibility via spin-strain coupling of Mn<sub>B</sub><sup>4+</sup>. The second mechanism concerns Mn pairs coupled by the position-dependent exchange interaction.

**Introduction.** – SrTiO<sub>3</sub> (STO) and KTaO<sub>3</sub> (KTO) doped by manganese have attracted considerable attention exhibiting simultaneous spin and dipole glass behaviours with large non-linear magnetoelectric coupling [1–3]. Such "multiglass" systems extend non-trivially the frame of conventional multiferroicity and give new perspective for studies of the phenomenon and potential application in microelectronic devices.

Both STO and KTO are special representatives of the perovskite family of ABO<sub>3</sub> materials. They are incipient ferroelectrics (IF), i.e. they remain paraelectric down to zero temperature, but exhibit very large dielectric permittivity ( $\sim 20000$  and  $5000$  respectively) at low temperature due to the softening of a transverse optical mode that corresponds to B sub-lattice oscillations with respect to the almost static rest of the lattice.

The Mn impurities in STO may substitute both for Sr and Ti; they will be denoted as Mn<sub>A</sub> and Mn<sub>B</sub> respectively. Isolated impurities are paramagnetic, Mn<sub>B</sub> being an isotropic centre with formal valency Mn<sup>4+</sup>, and a spin  $S = 3/2$  [4], while Mn<sub>A</sub> which has valency 2+ and

$S = 5/2$ , is isotropic at  $T > 100$  K, and axial at low temperature [5]. According to the interpretation of ESR measurements [4,5], which were recently confirmed by density functional theory (DFT) calculations [6,7] and EXAFS experiments [8], the Mn<sub>B</sub> impurity resides in the octahedrally coordinated cubic position B of the perovskite lattice, and Mn<sub>A</sub> is displaced from A position thus forming electric dipoles in addition to magnetic ones.

Ceramic samples of STO doped by 2% of manganese exhibit spin- and polar- glass properties at temperature below  $T_g \approx 38$  K. Moreover, a substantial non-linear magnetoelectric coupling was measured [1–3]. A similar behaviour for KTO:Mn system was also found [3]. The interaction of electric dipoles formed by off-central Mn<sub>A</sub> impurities has the same nature as the interaction of other dipole impurities in IF, its mechanism is rather well understood [9]. In this paper we concentrate on magnetic and magnetoelectric interactions in STO:Mn. We show that the presence of off-central Mn<sub>A</sub><sup>2+</sup> ions substituting for Sr is necessary but not sufficient to induce the multiglass behaviour, and that the magnetic interactions are medi-

ated by  $\text{Mn}_B^{4+}$  ions substituting for Ti.

Some aspects of the considered problem are interesting from the fundamental point of view. The interaction between ions with different  $d$ -shell filling and different spins connected by several bridging ligands requires a generalization of superexchange theory. The dependence of spin-Hamiltonian parameters on the external electric field is a non-trivial application of the ligand field theory for ions in a highly polarizable medium.

**Experiment.** – For our experimental studies we have used two groups of STO:Mn ceramic samples prepared in different labs. We will call them I and II. Type-I ceramics with the formal chemical composition  $\text{Sr}_{0.98}\text{Mn}_{0.02}\text{TiO}_3$  were prepared by mixed oxide technology described elsewhere [10]. In particular, reagent grade  $\text{SrCO}_3$ ,  $\text{TiO}_2$  and  $\text{MnO}_2$  were mixed in appropriate amounts, ball milled, dried and calcined at  $1100^\circ\text{C}$  for 2 h. The calcined powders were again milled, pressed isostatically and sintered at  $1500^\circ\text{C}$  for 5 h. For the type-II ceramics (formal chemical composition  $\text{Sr}_{0.96}\text{Mn}_{0.04}\text{TiO}_3$ ), instead of  $\text{MnO}_2$ , powder of  $\text{MnCO}_3$  was used. The calcination was performed at  $1150^\circ\text{C}$  for 4 h and the sintering at  $1360^\circ\text{C}$  for 2 h. Both types of samples possess  $\text{Mn}_A^{2+}$  off-central impurities and have similar dielectric properties, but as shown below their magnetic responses are strikingly different.

The magnetic measurements were performed using a SQUID magnetometre (MPMS-6S Quantum Design) in the temperature range 4.5 - 100 K. The zero-field-cooled (ZFC) and field-cooled (FC) susceptibilities were measured in an applied field of 100 Oe. The main experimental result of this paper is illustrated in Fig.1. While magnetic properties of type-I ceramics are similar to that reported in Refs. [1, 2], namely, they exhibit spin-glass behaviour at  $T < 45$  K (Fig. 1a), the type-II ceramics remain paramagnetic down to liquid helium temperature (Fig. 1b). In addition, for the ceramics I the magnetization exhibits a hysteretic behaviour with a finite remanence and coercivity (Fig. 1c). On the contrary, the magnetic loops measured on ceramics II (Fig. 1d) show no hysteresis and remanence. In this case, the magnetization is almost entirely determined by the paramagnetic contribution.

In order to study the distribution of Mn ions in the lattice and their individual magnetic properties -they are the only source of magnetism in our system- we have performed ESR measurements at 9.2 GHz in the standard 3 cm wavelength range at temperatures from 4.2 up to 300 K. An Oxford instrument ESR 900 cryosystem was used. In both types of ceramics we have found the spectra of  $\text{Mn}_A^{2+}$  and  $\text{Mn}_B^{4+}$  ions, which were described in detail in our previous paper and other early publications (see, e.g. Refs. [4,5]). The main difference between the two types of ceramics revealed by ESR is the ratio of  $\text{Mn}^{2+}/\text{Mn}^{4+}$  ion concentration, which is 70/30 and 90/10 for types I and II respectively, as shown in Fig. 1.e-h. The absolute concentration of  $\text{Mn}_A^{2+}$  in both ceramics is about  $1\div 1.3\%$  as the ceramics contain also some amount of  $\text{MnTiO}_3$  inclu-

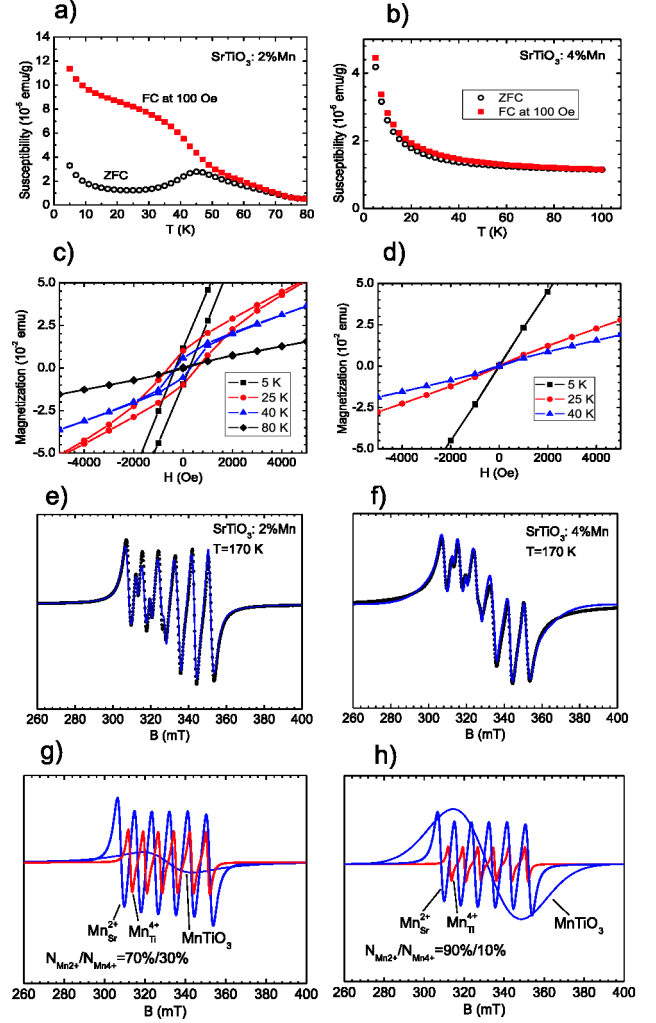


Figure 1: (Coloronline) Comparison of magnetic properties for ceramics I (left) and II (right). a),b) ZFC and FC susceptibilities as a function of temperature. Magnetization as a function of applied field, measured c) in type-I ceramics at 80, 40, 25, and 5 K, and d) in type-II ceramics at 40, 25, and 5 K. e),f) Experimental (dots) EPR spectra, and the corresponding simulations (solid lines). g),h) EPR spectra decomposition which shows the percentage of various Mn paramagnetic centres.

sions reflected in ESR spectra by a broad line (see, Fig. 1 g,h) and observed previously in electron diffraction spectra (Ref. [10]). Although in the type-II ceramics about 70% of Mn ions contribute to this  $\text{MnTiO}_3$  fraction, it does not markedly influence the magnetic properties of the studied samples (Figs. 1b,1d) due to relatively small magnetic anomaly of  $\text{MnTiO}_3$  at the antiferromagnetic phase transition at 63 K (Ref. [11]).

**DFT calculations.** – We have theoretically studied the interactions between Mn ions using LSDA+ $U$  and many-body perturbation theory. We have considered the Mn impurities when they occupy nearest neighbour positions, and looked at the various pairs  $\text{Mn}_A\text{-Mn}_A$ ,  $\text{Mn}_A\text{-Mn}_B$ , and  $\text{Mn}_B\text{-Mn}_B$ . The  $\text{Mn}_A$  ions were shifted in var-

Table 1: Hamiltonian (1) parameters calculated with LSDA+ $U$  for various configurations of  $\text{Mn}_A^{2+}$ - $\text{Mn}_A^{2+}$  pair in a  $2 \times 2 \times 3$  60 atom supercell (symmetry group P4mm, #99);  $U = 4$  eV

$d_1, \text{\AA}$	$d_2, \text{\AA}$	$E_n, \text{meV}$	$J_{AA}, \text{meV}$
0	0	0	-0.008
0.82	0.82	-695.5	0.23
0.35	-0.35	-26.6	0.46
-0.47	0.47	-27.2	0.04

ious directions from the symmetric A position.

Density functional theory calculations were performed using the full-potential local-orbital (FPLO) code [12]. The total energies for different configurations were obtained, and the results were mapped onto an Mn-Mn pair effective Hamiltonian of the form

$$\hat{H} = E_n(\mathbf{d}_1, \mathbf{d}_2) + J_{12}(\mathbf{d}_1, \mathbf{d}_2) \hat{\mathbf{S}}_1 \hat{\mathbf{S}}_2, \quad (1)$$

where  $\mathbf{d}_i$  is the shift from cubic position.  $E_n$  is a non-magnetic spin-independent interaction, treating the ion motion classically, it is a  $c$ -number in our approach. The spin part of the interaction is of Heisenberg-type.

We present the results for  $\text{Mn}_A^{2+}$ - $\text{Mn}_A^{2+}$  pairs in Table 1. Various  $\text{Mn}_A^{2+}$  displacements along the symmetry axis  $Z$  were considered:  $d_1 = d_2$  (the ions shift conserving the distance between them),  $d_1 = -d_2 > 0$  (ions shift towards each other),  $d_1 = -d_2 < 0$  (away from each other). In each case the results correspond to the total energy minima with respect to displacement. The non shifted distance between two A sites is 3.9 Å [6].

The third column shows that the configuration with parallel shift of Mn ions ( $d_1 = d_2 = 0.82\text{\AA}$ ) is separated from the others by such a large energy, that these will not be observed within the physically relevant temperature range. A similar situation was described in Ref. [15] for Li-Li pairs in  $\text{KTaO}_3$ . The last column of Table 1 represents one of the main theoretical findings of this work, namely, it shows that the magnetic interaction of nearest neighbour  $\text{Mn}_A^{2+}$  ions, for the most probable parallel configuration, satisfies  $|J_{AA}/k_B| < 3$  K. In fact this value is on the verge of precision of DFT calculations. Despite the large spin value of  $\text{Mn}_A^{2+}$  ions, this interaction cannot be responsible for magnetic susceptibility anomalies at  $T \sim 40$  K that we observe for type I ceramics (Fig.1), and that were reported in previous studies of STO:Mn [1, 2].

Table 2 shows the results for a  $\text{Mn}_A^{2+}$ - $\text{Mn}_B^{4+}$  pair. Here the  $\text{Mn}_A^{2+}$  ion shift was taken to be the same as the one found for the isolated ion [6]; for  $d_A > (<)0$  the ions get farther (closer). Finally, for the pair  $\text{Mn}_B^{4+}$ - $\text{Mn}_B^{4+}$  we have found  $J_{BB} = 9.3$  meV, i.e.  $J_{BB}/k_B = 107.9$  K. So, we may conclude that the presence of  $\text{Mn}_B^{4+}$  ions may be responsible for the observed anomalies in magnetic susceptibilities.

**Theory of superexchange.** – To reach a better understanding of the exchange mechanism we have per-

Table 2: Hamiltonian parameters for  $\text{Mn}_A^{2+}$ - $\text{Mn}_B^{4+}$  pair, calculated for a  $2 \times 2 \times 2$  40 atom supercell (P1, #1);  $U = 4$  eV

$d_A, \text{\AA}$	$E_n, \text{meV}$	$J_{AB}, \text{meV}$	$J_{AB}/k_B, \text{K}$
0	0	0.5	5.8
-0.64	-144.6	1.65	19.1
0.64	-123.02	0.51	5.9

formed analytic calculations of the superexchange interaction between Mn ions within fourth-order many-body perturbation theory. Using resolvent method [16] we obtained a general formula for the magnetic coupling between two spins  $S_1$  and  $S_2$  in terms of hopping integrals  $t_{im\beta n}$  between cations ( $im$ ) ( $i$  specifies the cation,  $m$  the orbital index) and neighbouring ligands ( $\beta n$ ) ( $\beta$  specifies the ligand,  $n$  the orbital). Taking the hole point of view (no fermion on the ligand  $p$  orbitals in the ground state) we have established Eq.(2), where the sum over the cation orbitals  $m$  and  $m'$  is restricted to ground-state occupied ones (abbreviation "occ").  $\Delta_{i\beta n}$  is the energy of the excited state (measured with respect to the ground state), where one fermion has moved from ( $im$ ) to ( $\beta n$ ), while  $\Delta_{ij}$  is the difference of energy between an excited state with  $N_i - 1$  and  $N_j + 1$  fermions on cation  $i$  and  $j$  respectively, and the ground state (GS) with  $N_i$  and  $N_j$  fermions per cation respectively. If the cations are of the same type, one has  $\Delta_{ij} = \Delta_{ji}$  and  $\Delta_{i\beta n}$  does not depend on  $i$ . The three added terms inside the bracket in Eq.(2) correspond to different paths: the first two involve intermediate excited states with  $(N_i - 1, N_j + 1)$  fermions on the cations, while the third term corresponds to an excited state with two fermions on the ligands with repulsion  $U_p$  when the holes meet on the same ligand.

The parameters  $t_{im\beta n}$ ,  $\Delta_{i\beta n}$  and  $\Delta_{ij}$  were extracted from the analysis of photoemission experiments reported in Refs. [17, 18]. We denote for the BB-pair:  $\Delta_{12} = U_{eff}^B$ ,  $\Delta_{i\beta n} = \Delta_{eff}^B$ ; for the AA-pair  $\Delta_{12} = U_{eff}^A$ ,  $\Delta_{i\beta n} = \Delta_{eff}^A$ ; while for the BA-pair  $\Delta_{12} = \Delta_{eff}^B - \Delta_{eff}^A + U_{eff}^A$ ,  $\Delta_{21} = \Delta_{eff}^A - \Delta_{eff}^B + U_{eff}^B$ ,  $\Delta_{1\beta n} = \Delta_{eff}^B$ , and  $\Delta_{2\beta n} = \Delta_{eff}^A$ , where  $\Delta_{eff}^i = \Delta_i + J_{Hi} [7/9(N_i - 1) - p_i]$  and  $U_{eff}^i = U_i + J_{Hi} [N_i + 11/9 - 2p_i]$ , with  $J_{Hi} = 5/2B_i + C_i$ ,  $N_i$  is the number of holes in the ground state of  $\text{Mn}_i$  ion and  $p_i$  is the number of doubly-occupied orbitals. We use the following experimental values (in eV) for  $\text{Mn}_B$ :  $B_i = 0.132$ ,  $C_i = 0.610$ ,  $\Delta_i = 2 \pm 0.5$  and  $U_i = 7.5 \pm 0.5$  (Table I of Ref. [17]), while for  $\text{Mn}_A$ ,  $B_i = 0.119$ ,  $C_i = 0.412$ ,  $\Delta_i = 7$  and  $U_i = 5.5$  (Table I, II of Ref. [18]). This gives  $\Delta_{eff}^A = 9.2\text{eV}$ ,  $\Delta_{eff}^B = 4.5 \pm 0.5\text{eV}$ ,  $U_{eff}^A = 9.9\text{eV}$  and  $U_{eff}^B = 11.6 \pm 0.5\text{eV}$ . The hopping parameters are expressed in terms of Slater-Koster parameters [19]  $V_{pd\pi, \sigma}^{A(B)}$  for  $\text{Mn}_{A(B)}$ , they essentially depend on the cation-ligand distance, we take  $V_{pd\sigma}^i/V_{pd\pi}^i = -2.16$  [19]. Following Ref. [18], we have assumed that the hopping which links states

$$\begin{aligned}
J = & \frac{1}{2S_1S_2} \sum_{\beta\beta'nn'} \sum_{mm'}^{occ} t_{1m\beta n} t_{2m'\beta n} t_{1m\beta'n'} t_{2m'\beta'n'} \left\{ \frac{1}{\Delta_{1\beta n} \Delta_{1\beta'n'} \Delta_{12}} + \frac{1}{\Delta_{2\beta n} \Delta_{2\beta'n'} \Delta_{21}} \right. \\
& \left. + \frac{1}{\Delta_{1\beta n} + \Delta_{2\beta'n'} + U_p \delta_{\beta\beta'}} \left( \frac{1}{\Delta_{1\beta n}} + \frac{1}{\Delta_{2\beta'n'}} \right) \left( \frac{1}{\Delta_{2\beta n}} + \frac{1}{\Delta_{1\beta'n'}} \right) \right\}, \quad (2)
\end{aligned}$$

Table 3: Superexchange values  $j_{BA} = J_{BA}/J_{BB}$ , and  $j_{AA} = J_{AA}/J_{BB}$  with  $J_{BB} = (9.5 \pm 1.5)(V_{pd\pi}^B)^4$  for different A-shift.

$d_A$	$j_{BA}$	$j_{BA},$ LSDA+U	$j_{AA}$	$j_{AA},$ LSDA+U
0	0.39	0.054	0.008	-0.001
0.82			0.008	0.025
-0.64	0.52	0.177		
0.64	0.29	0.055		

with  $N + 1$  and  $N$  holes on some cation, is reduced by a factor  $R$  compared to hopping linking states with  $N - 1$  and  $N$  holes. The results (and their comparison with LSDA+U) are presented in Table 3 for the parameters  $R = 1.2$  and  $U_p = 4$  eV, and the shifts are the same as those found in LSDA calculations.

As can be seen, the agreement is qualitative between perturbative calculations and DFT results. In addition, the super-exchange theory enables to discuss various tendencies and contributions. The different exchange coupling  $J_{BB}$ ,  $J_{AB}$  and  $J_{AA}$  are proportional to  $(V_{pd\pi}^B)^4$ ,  $(V_{pd\pi}^A)^2(V_{pd\pi}^B)^2$  and  $(V_{pd\pi}^A)^4$  respectively. A crude estimate based on the different distances, leads to  $J_{AB}/J_{BB} \sim 0.1$  and  $J_{AA}/J_{BB} \sim 0.01$ . One can also expect a predominant value for  $J_{BB}$  due to geometry: it corresponds to a  $180^\circ$  Mn<sub>B</sub>-O-Mn<sub>B</sub> link, while the other two are  $90^\circ$  ones. The difference between exchange couplings are also due to different number of exchange paths and to difference in charge transfer values  $\Delta_{eff}^A > \Delta_{eff}^B$ . The number of paths for  $J_{AA}$  is larger than for the other two, since four ligands and many orbitals come in, against three ligands for  $J_{AB}$  and only one for  $J_{BB}$ . Two or more ligands raise the opportunity to have ferromagnetic contributions, which explains reduction of  $J_{AA}$  compared to the other two, further than what was expected just by distance effect.

#### Mechanisms of magnetoelectric coupling. –

We propose two possible mechanisms involving Mn<sub>B</sub><sup>4+</sup> ions, which may be relevant for IF doped by manganese. In the following we consider the solid solution Sr<sub>1-x</sub>Mn<sub>x</sub>Ti<sub>1-y</sub>Mn<sub>y</sub>O<sub>3</sub>. The magnetoelectricity implies the dependence of the magnetic susceptibility on an electric field. Up to second order, the magnetic susceptibility

may be written

$$\chi_{ij} = - \left. \frac{\partial^2 F}{\partial H_i \partial H_j} \right|_{H=0} = \chi_{0,ij} + \chi_{1,ijk} E_k + \chi_{2,ijkl} E_k E_l. \quad (3)$$

where the free energy density  $F$ , the magnetic and electric field components,  $H_i$  and  $E_i$  are measured in CGS units. To translate this equation in terms of Ref. [2] notations with SI units, one should use the relations

$$\begin{aligned}
\beta_{ijk} &= (4\pi)^{\frac{3}{2}} \mu_0 \sqrt{\varepsilon_0} \chi_{1,ijk} \approx 1.67 \cdot 10^{-10} \chi_{1,ijk} \text{ s/A} \quad (4) \\
\delta_{ijkl} &= 8\pi^2 \mu_0 \varepsilon_0 \chi_{2,ijkl} \approx 8.78 \cdot 10^{-16} \chi_{2,ijkl} \text{ sm/VA} \quad (5)
\end{aligned}$$

The first mechanism is a one-spin effect: The polarization  $P$  of the lattice, is accompanied by a lattice strain, which is proportional to the square of polarization [20]. The Mn<sub>B</sub><sup>4+</sup> ion has a  $3d^3$  configuration and a  $^4F$  GS, which is split by the ligand field in contrast to the  $3d^5$  configuration and  $^6S$  GS for Mn<sub>A</sub><sup>2+</sup>. In a cubic field the Mn<sub>B</sub><sup>4+</sup> ion has a fourfold degenerate  $^4A_2$  GS. When the local symmetry becomes axial, an additional splitting arises. Its magnitude depends on the polarization via the strain. This affects the magnetic susceptibility. In a paraelectric phase, the changes are proportional to the square of the external electric field, but in the presence of a net polarization  $P_T$  in a polar phase, a linear dependence appears. Let us note that this mechanism will be effective in any ferroelectric perovskite doped by paramagnetic ions located at B sites and having the  $3d^3$  configuration.

The contribution of this mechanism to the magnetoelectric susceptibility is given below by Eqs.(9) and (10). Substitution of numerical values relevant to the experimental conditions of Ref. [2] gives

$$\chi_{1,zzz} \approx -2.2 \cdot 10^{-9}, \quad \beta \approx -3.6 \cdot 10^{-19} \text{ s/A}, \quad (6)$$

$$\chi_{2,zzzz} \approx -1.2 \cdot 10^{-10}, \quad \delta \approx -0.1 \cdot 10^{-24} \text{ sm/VA}. \quad (7)$$

In these estimates, we have used  $x + y = 0.02$ , and  $x/y \approx 70/30$ , as found in our ESR experiment. The reported experimental values are [2]  $\beta \approx -3 \cdot 10^{-19}$  s/A and  $\delta \approx -9 \cdot 10^{-24}$  sm/VA. We see that the paramagnetoelectric susceptibility  $\beta$  is in fairly good agreement, but the biquadratic coefficient is underestimated by this mechanism which cannot be the only argument put forward.

The second mechanism concerns Mn<sub>A</sub>-Mn<sub>B</sub> pairs. As can be seen from Tables 2 and 3, the Mn<sub>A</sub><sup>2+</sup> has non-equivalent equilibrium positions in the cell where Mn<sub>B</sub><sup>4+</sup> is present. The superexchange interaction between Mn<sub>B</sub><sup>4+</sup> and Mn<sub>A</sub><sup>2+</sup> strongly depends on the displacement  $d_A$ .

Compared to the closer situation, the case with ions far from each other corresponds to a higher energy  $\Delta E$ . As shown in detail in the following section, the lattice polarization increases the number  $N_2(P_r, E)$  of  $\text{Mn}_A^{2+}$  ions lying farther from  $\text{Mn}_B^{4+}$  ions. This leads to a positive  $\chi_{1,zzz}$ . In the next section we show that this mechanism seems to be unimportant for the system studied in Ref. [2], but it may be very effective for a system where the interaction energy between electric  $\text{Mn}_A^{2+}$ -dipole and  $P_r$  is comparable with  $\Delta E$ .

**Calculation of non-linear magneto-electric susceptibility.** – Here we quantitatively consider the ideas outlined in the previous section. This section is a little technical and can be safely skipped by someone not interested in the details of computation.

*The first mechanism.* In order to estimate its contribution, we follow the ideas of Ref. [21]. The  $\text{Mn}_B^{4+}$  ion is much more sensitive to the local strain than  $\text{Mn}_A^{2+}$ . In an octahedral coordination it has a  ${}^4A_2$  orbital singlet ground state, and the effective spin 3/2 Hamiltonian has the form

$$\hat{H}_B = \mu_B g_{zz} H_z \hat{S}_z + \mu_B g_{\perp} (H_x \hat{S}_x + H_y \hat{S}_y) + D \left[ \hat{S}_z^2 - \frac{1}{3} S(S+1) \right] - \mu_B^2 \sum_{\mu\nu} \Lambda_{\mu\nu} H_{\mu} H_{\nu}, \quad (8)$$

where  $g_{\mu\nu} = g_s - 2\lambda k \Lambda_{\mu\nu}$ ,  $D = -\lambda^2 (\Lambda_{zz} - \Lambda_{xx})$ ,  $\Lambda_{\mu\nu} = \sum_{n \neq 0} \frac{\langle \psi_0 | \hat{L}^{\mu} | n \rangle \langle n | \hat{L}^{\nu} | \psi_0 \rangle}{E_n - E_0}$ ,  $g_s = 2.0023$  is the spin gyromagnetic ratio,  $\lambda$  the spin-orbit coupling constant,  $|\psi_0\rangle (|n\rangle)$  is the ground(excited) state,  $E_0$  and  $E_n$  are the corresponding energies,  $\hat{L}^{\mu}$  is the  $\mu$ -th component of the orbital moment operator,  $k$  is the orbital reduction factor. Using the ligand field theory [22,23], which perturbatively takes into account  $p-d$  hybridization between paramagnetic ion and surrounding ligands, we may obtain [24]

$$\Lambda_{zz} = -\Delta g_{cub} (1 - \kappa e_{33}) / 2\lambda, \\ \Lambda_{xx} = -\Delta g_{cub} (1 - 5\kappa e_{33}/2) / 2\lambda,$$

where  $\Delta g_{cub} = g_{cub} - g_s$  refers to the  $g$ -value for undistorted cubic lattice,  $\kappa \sim -3.5, -4$  is the exponent of  $p-d$  hopping dependence on distance [19]. The dependence on electric field of the previous equations is only in the strain  $e_{33}$ . For multiglass samples we may assume that both, the net polarization  $P_r$  and the electric field are directed along the axis  $Z$ , while  $\mathbf{P} = \mathbf{P}_r + (\varepsilon - 1) \mathbf{E} / 4\pi$ . With an external magnetic field also applied along the  $Z$ -axis, we compute the partition function  $Z_B$  and the free energy density  $F_B = -(y/v_c)\theta \ln Z_B$ , with  $y/v_c$  the density of  $\text{Mn}_B^{4+}$  ions,  $v_c$  the host lattice unit cell volume and  $\theta \equiv k_B T$ . From this free energy, we finally derive the linear contribution to the magnetic susceptibility (Eq.(3)):

$$\chi_{1,zzz} \approx -\frac{y}{v_c} \mu_B^2 \Lambda'_{zz} \left\{ \frac{g_{zz}\lambda}{\theta} \left[ 5k + \frac{3g_{zz}\lambda}{2\theta} \right] - 2 \right\}, \quad (9)$$

where we have taken into account that  $D/\theta \ll 1$  for  $T = 10$  K. The (double)-prime indicates the (second)-

derivative with respect to  $E$ . Similarly, for the second order contribution, we have

$$\chi_{2,zzzz} \approx \frac{y\mu_B^2}{v_c} \left\{ k (\lambda \Lambda'_{zz})^2 [10k + 12g_{zz}\lambda/\theta] / \theta - \Lambda''_{zz} \left[ \frac{g_{zz}\lambda}{\theta} \left( 5k + \frac{3g_{zz}\lambda}{2\theta} \right) - 2 \right] \right\}. \quad (10)$$

When we substitute  $\kappa = -3.5$ ,  $g_{cub} = 1.992$  [5],  $\lambda \approx 135$   $\text{cm}^{-1}$ , [25],  $k \approx 1$ , SrTiO<sub>3</sub> lattice parameter  $a = 3.9$   $\text{\AA}$ , ( $v_c = a^3$ ), and  $c/a \approx 1.002$  [6],  $\varepsilon(T = 10 \text{ K}) \approx 1500$ , and a net polarization  $P_r \approx 0.7$ ,  $\mu\text{C}/\text{m}^2 = 2100$   $\text{esu}/\text{cm}^2$  [10], we obtain the values presented in Eqs. (6) and (7).

*The second mechanism.* It involves a pair of  $\text{Mn}_A$ - $\text{Mn}_B$  ions. There are six available positions for  $\text{Mn}_A$ , three

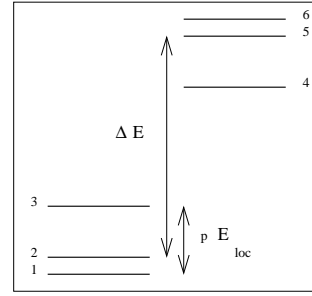


Figure 2: Changes of  $\text{Mn}_A$ - $\text{Mn}_B$  pair energies in polarized medium. Here  $E_{loc} = E + \frac{4\pi}{3}\gamma P$  is positive, however it can be negative, depending on the relative direction of polarization with respect to the pair  $\text{Mn}_A$ - $\text{Mn}_B$ . The Lorentz factor  $\gamma$  accounts for the deviation of the local field from the simple cubic case,  $p \approx Z_A d_A$  is the dipole moment of  $\text{Mn}_A^{2+}$ ,  $Z_A \approx 2$  is its dynamic charge.

of them are closer to  $\text{Mn}_B^{4+}$  and lower in energy: the number of  $\text{Mn}_A^{2+}$  in deep (shallow) wells is  $N_{1(2)}$ . Writing  $N_1 = n_1 + n_2 + n_3$ , and  $N_2 = n_4 + n_5 + n_6$ , one has in absence of polarization  $N_2/N_1 = \exp(-\Delta E/\theta)$ . However with polarization, there is some lift of degeneracy, as can be seen on Fig. 2, this leads to a redistribution of level occupancies, and  $N_{1(2)}$  acquires a dependence on the net polarization  $P_r$  and on the external electric field  $E$ . With  $N_1 + N_2 = xyz$ , ( $z = 8$  is the coordination number), the susceptibility reads

$$\chi = \chi_0 + \chi_1 xyz + (\chi_2 - \chi_1) N_2(P_r, E), \quad (11)$$

where  $\chi_0$  comes from contribution of everything but  $\text{Mn}_A$ - $\text{Mn}_B$  pairs, while  $\chi_J (J = 1, 2)$  is the susceptibility of a pair  $S_A = 5/2 - S_B = 3/2$  coupled by the exchange interaction  $J_{AB}(d_A)$ , which depends on the  $\text{Mn}_A$  position [26]. The dependence of  $\chi$  on the electric field comes from  $N_2(P_r, E)$ . Defining  $n(t) \equiv (2 + e^{-t})/(2 + e^t)$ , one has

$$N_2(P_r, E) = \frac{xyz}{2} \left[ \frac{1}{n(t)e^{\Delta E/\theta} + 1} + \frac{1}{n(-t)e^{\Delta E/\theta} + 1} \right] \quad (12)$$

with  $t = pE_{loc}/\theta$ ,  $pE_{loc} \approx cE + \Delta_r$ ,  $c = p\varepsilon\gamma/3$  and  $\Delta_r = 4\pi\gamma p P_r/3$ , ( $\varepsilon \gg 1$  was used). See the caption of Fig. 2 for

definitions. Finally, making a limited development up to second order in electric field  $E$ , we obtain

$$\chi_{1,zzz} = (\chi_2 - \chi_1) N_2'(P_r, 0), \quad (13)$$

$$\chi_{2,zzzz} = (\chi_2 - \chi_1) N_2''(P_r, 0). \quad (14)$$

Substituting the values from Table 2:  $\Delta E \approx -123 + 144.6 = 21.6$  meV,  $J_1 \approx 1.7$  meV,  $J_2 \approx 0.5$  meV, and  $\gamma \approx -0.2$  [9], this gives  $\Delta_r \approx -14$  meV, and a very tiny contribution of this second mechanism to the susceptibilities  $\chi_1 \approx 7.1 \cdot 10^{-15}$ ,  $\chi_2 \approx 1.6 \cdot 10^{-15}$ . However, since  $N_2'$  is strongly dependent on  $\Delta E - \Delta_r$ , the second mechanism could be of the same order than the first one or even exceed it for  $\Delta E \approx \Delta_r$  (then  $\chi_1 \approx 4.6 \cdot 10^{-7}$ ,  $\chi_2 \approx 1.7 \cdot 10^{-7}$ ): this equality can be realized for other concentrations of manganese in SrTiO<sub>3</sub> host, or for other systems (e.g. K<sub>1-x</sub>Mn<sub>x</sub>Ta<sub>1-y</sub>Mn<sub>y</sub>O<sub>3</sub> [3]).

**Summary.** – We have compared the magnetic properties of two types of ceramic samples of manganese doped SrTiO<sub>3</sub>. Based on the data of ESR measurements we conclude that the spin-glass behaviour is observed only in samples containing an appreciable percentage of Mn<sub>B</sub><sup>4+</sup> ions substituting for Ti, in addition to Mn<sub>A</sub><sup>2+</sup> substituting for Sr. Using LSDA+ $U$  supercell calculation we have shown that the exchange interaction between Mn<sub>A</sub><sup>2+</sup> impurities is an order of magnitude smaller than those for Mn<sub>B</sub><sup>4+</sup>-Mn<sub>A</sub><sup>2+</sup> and Mn<sub>B</sub><sup>4+</sup>-Mn<sub>B</sub><sup>4+</sup> pairs. The analytic many-body calculations have shown that the reason for this difference is the interference of various exchange paths for the Mn<sub>A</sub><sup>2+</sup>-Mn<sub>A</sub><sup>2+</sup> pairs combined with different geometry, Mn-O distances, and stability of the Mn<sub>A</sub><sup>2+</sup> ground state configuration in comparison to other pairs. We conclude that the presence of Mn<sub>B</sub><sup>4+</sup> ions is essential for the formation of a collective magnetic state at low temperature. We propose two microscopic mechanisms of magnetoelectricity in SrTiO<sub>3</sub>:Mn which involve Mn<sub>B</sub><sup>4+</sup> ions.

\* \* \*

The authors thank M.D. Glinchuk for fruitful discussions, the PICS program (Contracts CNRS No. 4767, NASU No. 267) and grant MSMT CR (Project No. 1M06002) for financial support and the IFW Dresden (Germany) which allowed us to use their computer facilities. The institutional research plan AVOZ10100521 is acknowledged.

## References

- [1] KLEEMANN W., SHVARTSMAN V. V., BEDANTA S., BORISOV P., TKACH A. and VILARINHO P. M., *J. Phys.: Cond. Matt.*, **20** (2008) 434216.
- [2] SHVARTSMAN V. V., BEDANTA S., BORISOV P., KLEEMANN W., TKACH A. and VILARINHO P. M., *Phys. Rev. Lett.*, **101** (2008) 165704
- [3] KLEEMANN W., BEDANTA S., BORISOV P., SHVARTSMAN V. V., MIGA S., DEC J., TKACH A. and VILARINHO P. M., *Eur. Phys. J. B*, **71** (2009) 407
- [4] MULLER K.A., *Phys. Rev. Lett.*, **2** (1959) 341; MULLER K. A., and BURKARD H., *Phys. Rev. B*, **19** (1979) 3593
- [5] LAGUTA V. V., KONDAKOVA I. V., BYKOV I. P., GLINCHUK M. D., TKACH A., VILARINHO P. M., and JASTRABIK L., *Phys. Rev. B*, **76** (2007) 054104
- [6] KONDAKOVA I. V., KUZIAN R. O., RAYMOND L., HAYN R., and LAGUTA V. V., *Phys. Rev. B*, **79** (2009) 134117
- [7] O. E. KVYATKOVSKI, *Phys. Solid State*, **51** (2009) 982
- [8] LEVIN I., KRAYZMAN V., WOICIK J. C., TKACH A., and VILARINHO P. M., *Appl. Phys. Lett.*, **96** (2010) 052904
- [9] VUGMEISTER B. E. and GLINCHUK M. D., *Rev. Mod. Phys.*, **62** (1990) 993
- [10] TKACH A., VILARINHO P. M., and KHOLKIN A. L., *Appl. Phys. Lett.*, **86** (2005) 172902; TKACH A., VILARINHO P. M., and KHOLKIN A. L., *Acta Mater.*, **53** (2005) 5061
- [11] STICKLER J.J., KERN S., WOLD A., and HELLER G.S., *Phys. Rev.*, **164** (1967) 765
- [12] FPLO-7.00-28 (improved version of the original FPLO code by KOEPERNIK K. and ESCHRIG H., *Phys. Rev. B*, **59** (1999) 1743; <http://www.FPLO.de>). The exchange and correlation potential of Perdew and Wang [13] was employed as well as the FPLO implementation of LSDA+ $U$  method in the atomic limit scheme [14].
- [13] PERDEW J. P. and WANG Y., *Phys. Rev. B*, **45** (1992) 13244
- [14] ESCHRIG H., KOEPERNIK K., and CHAPLYGIN I., *J. Solid State Chem.*, **176** (2003) 482
- [15] PROSANDEEV S.A., COCKAYNE E., and BURTON B.P., *Phys. Rev. B*, **68** (2003) 014120
- [16] AUERBACH A., *Interacting electrons and quantum magnetism* (Springer-Verlag) 1994
- [17] BOCQUET A. E., MIZOKAWA T., SAITOH T., NAMATAME H., and FUJIMORI A., *Phys. Rev. B*, **46** (1992) 3771
- [18] MIZOKAWA T., and FUJIMORI A., *Phys. Rev. B*, **48** (1993) 14150
- [19] HARRISON W.A., *Electronic structure and the Properties of Solids* (Freeman (San Francisco)) 1980
- [20] RIMAI L. and DEMARS G. A., *Phys. Rev.*, **127** (1962) 702
- [21] HOU S. L. and BLOEMBERGEN N., *Phys. Rev.*, **138** (1965) A1218
- [22] KUZMIN M.D., POPOV A.I., and ZVEZDIN A.K., *Phys.Stat. Sol. (b)*, **168** (1991) 201
- [23] KUZIAN R.O., DARÉ A.M., SATI P., and HAYN R., *Phys. Rev. B*, **74** (2006) 155201
- [24] GLINCHUK M.D., and KUZIAN R.O., *Physica B*, **389** (2007) 234
- [25] ABRAGAM A. and BLEANEY B., *Electron Paramagnetic Resonance of Transition Ions* (Clarendon, Oxford) 1970, p. 437
- [26] We have

$$\chi_J = \sum_{S=|S_A-S_B|}^{|S_A+S_B|} \frac{(2S+1) \exp(-E_S/\theta)}{\sum_{S'} (2S'+1) \exp(-E_{S'}/\theta)} \chi_S \quad (15)$$

with  $E_S = \frac{1}{2} J_{AB} [S(S+1) - S_A(S_A+1) - S_B(S_B+1)]$ , the magnetic energy of the pair corresponding to the total spin  $S$ ,  $\chi_S = (\mu_B g_S)^2 S(S+1) / (3v_c \theta)$  is the corresponding magnetic susceptibility, and the gyromagnetic ratio is  $g_S = \frac{1}{2} \left[ g_A + g_B + (g_A - g_B) \frac{S_A(S_A+1) - S_B(S_B+1)}{S(S+1)} \right]$ .